Evaluation of Low-Loss Polymer Switches for Multinuclear MRI/S*

Edith Touchet-Valle, *Student Member, IEEE*, Seelay Tasmim, Taylor H. Ware, and Mary P. McDougall, *Senior Member, IEEE*

***Abstract*— Implementation of multinuclear MRI/S as a diagnostic tool in clinical settings faces many challenges. One of those challenges is the development of highly sensitive multinuclear RF coils. Current multi-tuning techniques incorporate lossy components that impact the highest achievable SNR for at least one of the coil frequencies. As a result, optimization of multinuclear coil designs continues to be a priority for RF hardware engineers. To address this challenge, a new frequency switching technology that incorporates stimuli-responsive polymer materials was explored. Q measurements were used as a comparison metric between single-tuned, a standard switching network, and the proposed switching technology. The Q losses measured in the new switching method remained below 38% when compared to single-tuned coils. These results are consistent with low loss values reported using traditional switching networks. Furthermore, preliminary testing indicates that there is potential for improvement. These results establish the new technology as a promising alternative to traditional switching techniques.**

***Clinical Relevance*— A low loss multi-tuning technique for MRI radiofrequency coils has the potential of improving the study and diagnosis of disease.**

I. Introduction

Magnetic Resonance Imaging and Spectroscopy (MRI/S) are powerful non-invasive diagnostic tools that enable access to a wealth of chemical and physical information. In clinical settings, these tools are primarily used to assess structural and functional information from hydrogen (^{1}H) in the body. The use of non-^{1}H nuclei, also known as X-nuclei, can provide biochemical information that has the potential to further improve the study and evaluation of disease [1]. However, implementing X-nuclei MRI/S requires developing specialized hardware, including multinuclear radiofrequency (RF) coils [1, 2]. The development of RF coils is challenging because they must be highly sensitive to enable the detection of low gamma, less abundant X-nuclei. Several multi-tuning methods have been investigated and reported in the literature. Some of these methods include utilizing LC/LCC traps or switches in single-structure coils [3, 4]. Unfortunately, these methods of multi-frequency tuning involve the incorporation of lossy components that hinder coil sensitivity [5]. With the incorporation of such components, switching configurations specifically, have reported high losses in bench measurements and in SNR. Lim *et al.* reported losses of 75% in Q and 45% in SNR for the worst-case nucleus in comparison with single-tuned coils [6]. Choi *et al*. reported losses of 25% in Q_{ratio} and 30% in SNR for the worst-case nucleus when compared to a single-tuned coil [4].

The development of low-loss multi-tuning networks continues to be a goal in MRI/S. The application of switching between nuclei/frequencies fortunately has the advantage of not requiring high switching speeds – just the ability to co-register the data and not switch coils/move the subject. As a result, in this work, we explore the use of liquid crystal elastomers (LCEs) as a low-loss, novel switching method for multinuclear RF coils. LCEs are a class of novel materials that can undergo large, reversible, and programmed shape change over a period of seconds in response to MR compatible stimuli such as light [7-9]. The proposed switching method uses remote infrared light for actuation and liquid metal (LM) as the conductive element in the switch.

II. Methods

A. Hardware and Materials

A total of seven RF coils were developed for testing. The coils were 4 cm loops built using 18 AWG enameled copper wire (8049, Belden). The circuit networks were milled on single and double-sided 1 oz copper clad FR4 boards using a circuit milling system (LPKF Protomat S63). Fixed (111C Series, Passive Plus) and variable (SGC3S Series, Sprague-Goodman) capacitors were used on the networks to achieve tuning and matching. The networks that incorporated the LCE switching system were designed with breaks in the trace paths for the LCE to fill when actuated. On the other hand, the network with standard switching technology incorporated a PIN diode (MA4P7470F, MACOM), RF chokes (1812LS, Coil Craft), and DC lines for biasing. The DC lines were powered through an in-house bias board consisting of a current-limiting resistor (CRCW0402 Series, Vishay) and an RF choke.

The LCE material was synthesized via a two-step thiol-ene "click" reaction [10, 11]. Synthesis and material processing was carried out following previously published methods [12]. To enable LCE actuation with near-infrared (NIR) light illumination, 0.4 wt% of light absorbing carbon black particles were embedded in the polymer [12, 13]. The composite LC oligomer mixture was placed in a stainless-steel reservoir and loaded into the TAM-15 extruder printhead attachment of a

*Research supported by NIH grant R01EB028533 and R01EB028533-02S1.

Edith Valle is with the Department of Electrical and Computer Engineering, Texas A&M University, College Station, TX 77840 USA (e-mail: edithvvalle@tamu.edu).

Seelay Tasmim is with the Department of Biomedical Engineering, Texas A&M University, College Station, TX 77840 USA (e-mail: seelaytasmim@tamu.edu).

Taylor Ware is with the Departments of Biomedical Engineering and Materials Science & Engineering, Texas A&M University, College Station, TX 77840 USA (e-mail: taylor.ware@tamu.edu).

Mary P. McDougall is with the Departments of Biomedical Engineering and Electrical and Computer Engineering, Texas A&M University, College Station, TX 77840 USA (phone: 979-845-2421, e-mail: mpmcdougall@tamu.edu).

System 30M 3D printer (Hyrel ED, Norcross, GA). A 24G stainless steel dispensing needle with an inner diameter of 310 µm was attached to the reservoir nozzle. The material was printed as a disk with 0.6 mm thickness and 10 mm diameter. An Archimedean chord pattern was used to align LCE material while printing which resulted in LCE disks that, upon actuation, morphed into a cone [14]. Finally, a droplet of the liquid metal alloy eutectic gallium indium (EGaIn) was placed on the center of the LCE.

A custom testing platform was developed to combine the different elements of the switching technology in a consistent manner. The platform was made of three plexiglass stages aligned on top of each other (Fig. 1). The third level (bottom stage) contained an NIR chip on board LED (Luminus Devices, Inc., CBM-120) for LCE actuation. The second level consisted of a glass slide holder to place the LCE 1 cm away from the third level. At this distance, the light intensity of the LED was varied between 100-250 mW/cm^2 depending on the desired level of actuation of the LCE. The top level was a holder for placement of the RF coil in alignment with the LCE and the LM.

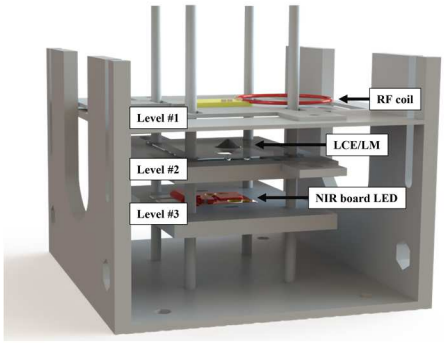

Figure 1. Schematic of the test platform for the LCE coils. Level #1 contains the RF coil. Level #2 contains the LCE and liquid metal switch. Level #3 contains the NIR chip on board LED device.

B. LCE Switch Preliminary Evaluation

Preliminary evaluation of the switching system tested the ability of the LCE and LM to complete a connection. A double-loop pick-up probe was placed 2 cm from the surface of level 1 on the test platform. The pick-up probe was connected to a network analyzer (Agilent Technologies E5071C) in an S_{21} configuration. Two 4 cm comparison coils were resonated to the ^{1}H frequency at 3T (128 MHz) for testing: 1) Coil R-Ref was a standard resonant loop coil, and 2) Coil R-LCE was identical but had an open trace path between one end of the loop and the tuning capacitors to eventually be closed by the LCE.

The performance of Coil R-LCE and the switching system was evaluated by comparing bench measurements with a reference and positive control. In each test case, the coils were placed on the test platform and compared under the same testing conditions, i.e., the NIR light was ON and the LCE switch was present and actuated. Three test cases were performed with these coils:

- Test Case #1: Coil R-Ref was used as the reference coil. The coil was placed on the testing platform, and the LCE was actuated using the NIR light. The LCE actuation was limited (light intensity: 100 mW/cm^2), so the LM drop would not contact the coil network.
- Test Case #2: Coil R-LCE was placed on the testing platform in the same manner. For this test, the LCE was fully actuated (light intensity: 250 mW/cm^2), so the LM drop connected the discontinued trace path on the board.
- Test Case #3: For the positive control (PC), the discontinued trace path on Coil R-LCE was connected using copper tape to represent the ideal outcome of testing (Coil R-PC). The coil was once again placed on the platform, and the LCE was actuated. The LCE actuation was limited (light intensity: 100 mW/cm^2) to prevent LM contact with the coil network.

The coils used in each of the three test cases are shown in Fig. 2. S_{21} and Q measurements were recorded for each test case. The percent change for test cases #2 and #3 was calculated with respect to Coil R-Ref.

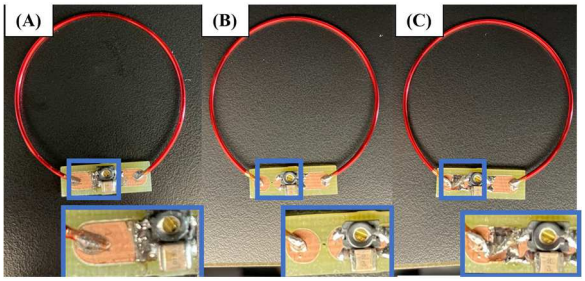

Figure 2. Resonant loop coils. (A) Standard resonant coil (R-Ref). (B) Resonant coil with open trace path to be completed with LCE switch (R-LCE). (C) Resonant coil with open trace path connected using copper tape (positive control – R-PC).

The LCE/LM was evaluated for its switching capability by implementing it to detune a ^{1}H single-tuned coil. The tune and match network was designed on a double-sided board. The network design is shown in Fig. 3. The bottom side consisted of two individual traces that were connected to each end of the coil loop via through-holes. The purpose of the traces was to short across the tuning capacitor to detune the coil when connected. The coil was connected to port 1 of the network analyzer (NA) in an S_{11} configuration and placed on the platform as described previously. The LCE was actuated with the NIR light to enable connection between the LM and the copper traces.

C. Multifrequency Switching Design and Performance

Four coils were used for testing the potential of the LCE to enable multifrequency coils via switching. The first two coils were single-tuned coils (Coil-ST), one for ^{1}H and the other for the additional X-nuclei frequency. In this case, phosphorous (^{31}P), with a frequency of 51.7 MHz at 3 T, was chosen as the second nucleus. The third coil (Coil-DT-LCE) was designed to be connected with the LCE. Finally, the fourth coil (Coil-DT-D) was designed with an identical network as the LCE coil but achieved frequency switching using a standard PIN diode configuration. The switching connections on Coil-DT-D were adjusted to account for the addition of the PIN diode, the RF choke, and the DC lines.

The switching networks were designed in a similar configuration to work previously reported by our group [15]. The network design for both coils is shown in Fig. 3.

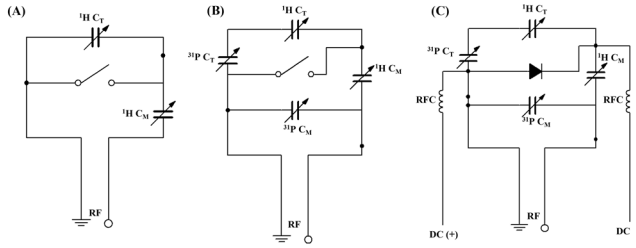

Figure 3. Switching network design. (A) Schematic for single-tuned coil with open trace to be detuned by LCE-LM switch. (B) LCE coil (Coil-DT-LCE) with open trace to switch frequency with LCE-LM switch. (C) Schematic for PIN diode coil (Coil-DT-D) with an identical network but replacing open trace with switching circuitry.

The networks were implemented on double-sided boards. The placement of the bottom traces was designed to avoid the introduction of capacitance between the top and bottom layers. Additionally, the networks were designed to minimize the number of connections needed to switch frequency. In this way, the undesired creation of additional potentially resonant loops was minimized as much as possible.

All four coils were placed on the testing platform and evaluated using Q measurements. Furthermore, as done previously, a positive control coil was created by completing the connection of Coil-DT-LCE using copper tape (Coil-DT-PC). The percent change between the single-tuned and switching coils was calculated.

III. Results and Discussion

A. Hardware and Materials

The testing platform successfully contained and aligned the components in the system. In future developments of this technology, a compact and enclosed setup will be needed to encase the LCE switch. Furthermore, the NIR chip on board LED will be replaced with an MR-compatible light source that will enable out-of-bore activation.

The LCE was successfully actuated at different rates using different light intensities. For the current development, continuous light illumination is required to maintain LCE actuation. However, fixed shape deformation has been reported with the incorporation of azobenzene or hydrazone molecules in LCE networks [16, 17]. These shape deformations are reversible with time or with the application of a second stimulus, e.g., heat or light at a different wavelength.

B. LCE Switch Preliminary Evaluation

Table 1 lists the S_{21} and Q measurements of the resonant coil structures. The difference in Q between the LCE coil and the reference coil remained below 5%, which was considered negligible.

TABLE I. Resonant Coil Structures Bench Measurements

Coil	Bench Measurement		
	S_{21}	Q	Q % Change
Coil R-Ref	-24.2	312	-
Coil R-LCE	-25.4	297	-4.80%
Coil R-PC	-23.7	312	0.04%

The LCE/LM as a switch successfully detuned the single-tuned coil. Although this switch is not viable to be implemented as a detuning method due to the slow switching speed (20 s), its performance demonstrated its ability to interact with a circuit as planned. For a video of the performance of the LCE in a detuning configuration, visit https://youtu.be/eeY2k5XjjVs.

C. Multifrequency Switching Design and Performance

Matching of better than -29 dB was achieved for all tested coils. The S_{11} plots of each coil and frequency are shown in Fig. 4.

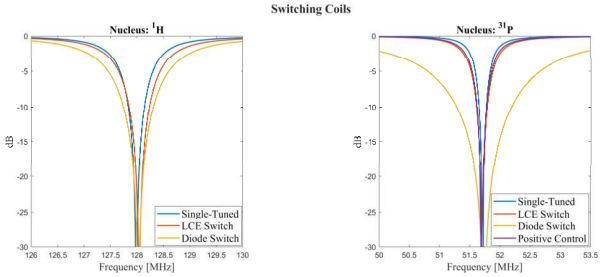

Figure 4. S_{11} plots of single-tuned and switching coils. (Left) Frequency: ^{1}H (128 MHz). (Right) Frequency: ^{31}P (51.7 MHz).

The LCE/LM switch before and after actuation, making full contact with a board, is shown in Fig 5.

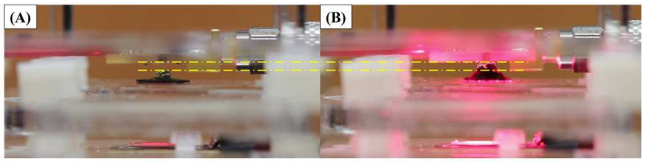

Figure 5. LCE switching system. Dotted lines showing the change in height in the LCE upon actuation. (A) LCE prior to actuation. (B) LCE after actuation and successful connection to the coil board.

The switching time for this test was approximately 60 s. The switching time can be decreased by placing the coil board closer to the LCE and adjusting the NIR light intensity. In this case, the actuation of the LCE was performed at a slower rate, and the coil was placed further away from the LCE for better viewing of the actuation. However, as demonstrated in the previous test case, the connection can be performed in 20 s. For a video showing frequency switching using the LCE, visit https://youtu.be/N7mkSHvJecY.

Table 2 shows the results of the bench measurements and calculated percent change between the reference, the positive control, and the switching coils. The decrease in Q between the single-tuned coils and the switching designs is expected due to the increased number of components, connections, and traces. As such, the positive control provided a better way to assess the performance of the LCE/LM on a similar coil.

TABLE II. BENCH MEASUREMENT RESULTS FOR ^{1}H AND ^{31}P COILS

Coil	Frequency: 128 MHz			Frequency: 51.7 MHz		
	Q	***Q* % Change (w.r.t.[b] Coil-ST)**	***Q* % Change (w.r.t.[b] Coil-DT-LCE)**	***Q***	***Q* % Change (w.r.t.[b] Coil-ST)**	***Q* % Change (w.r.t.[b] Coil-DT-LCE)**
Coil-ST (Single-Tuned)	291	N/A	N/A	323	N/A	N/A
Coil DT-PC (Positive Control)	N/A[a]	N/A	N/A	235	-27%	N/A
Coil-DT-LCE (LCE Switch)	228	-21%	N/A	199	-38%	-15%
Coil-DT-D (Diode Switch)	156	-46%	-32%	38	-88%	-84%

a. No positive control was needed for ^{1}H.
b. With respect to

During testing, it was noted that after placing all the components on a new tune and match board and cleaning it with isopropanol, the LM made better contact with the copper traces, resulting in higher Q. After repeated handling of the board and adjustment of connections with solder and liquid metal, the Q decreased to 199 for ^{31}P. Despite this issue, testing of the final board version resulted in the same Q measurement (199), as reported in Table 2, after testing with multiple connecting/disconnecting cycles. Although this Q value was 15% lower than the positive control, the coil performed substantially better than the coil with standard switching components (i.e., the PIN diode). The Q of the LCE switch coil was 32% higher for ^{1}H and 84% higher for ^{31}P than the diode switch coil. Even though the losses in Q in the PIN diode coil are consistent with similarly high Q losses (75%) observed in the literature [6], they are considered significant. This indicates that adjustments may be needed to improve coil performance. Adjustments to the switching circuitry design will be explored and evaluated.

Furthermore, the LCE switch to board distance and the light intensity will be improved for the implementation of the final version of the device. The actuation speed of the LCE is dependent on the intensity of the IR light triggering its shape change. In our experiment, we controlled the light intensity of the board LED by varying the supplied current. The light intensity at the surface of the LCE depends on the distance between the sample and the NIR LED. For these experiments, the distance between the light and the LCE switch were kept the same and light intensities were varied between 100-250 mW/cm^2 to adjust the actuation rate as needed for each experiment. NIR irradiation at low intensities are non-ionizing, non-thermal, and safe for human exposure [18, 19]. NIR light with low intensities is commonly used in photobiomodulation for simulation, healing, and regeneration of tissue [20]. Ferraresi et al., studied the therapeutic effects of NIR light with intensities ranging from 100 – 500mW/cm^2, and concluded that such light therapy could have therapeutic effects for athletes [21]. Although the system design in this study will be enclosed and we do not expect a subject to be exposed to the light, any potential exposure of light with intensities of 100 – 250mW/cm^2 is considered non-hazardous. These results showcase the potential of the proposed switching technology for coil multi-tuning for any field strength and combination of nuclei. Future work will focus on utilizing an MR-compatible light source (e.g., fiber optic cables connected to a remote light source) and enable placement of the switching system at various orientations. Imaging data will also be acquired to perform SNR comparisons and further assess the proposed switching technology. Furthermore, the final version of the switching design will be encased and isolated to prevent any changes or introducing impurities that may impact contact with LM.

IV. CONCLUSION

A new frequency switching method for multinuclear MRI/S was presented. The LCE switch was compared to standard switching technology, and performance consistent with low loss switching networks was demonstrated. Future work will focus on repeatability testing, adding more frequencies to the network, as well as incorporating MR-compatible elements for testing in a scanner.

REFERENCES

[1] G. Madelin, *X-Nuclei Magnetic Resonance Imaging*. Jenny Stanford Publishing Pte. Ltd., 2022, p. 466.

[2] R. Hu, D. Kleimaier, M. Malzacher, M. A. U. Hoesl, N. K. Paschke, and L. R. Schad, "X-nuclei imaging: Current state, technical challenges, and future directions," *Journal of Magnetic Resonance Imaging,* vol. 51, no. 2, pp. 355-376, 2020-02-01 2020, doi: 10.1002/jmri.26780.

[3] M. D. Schnall, V. Harihara Subramanian, J. S. Leigh, and B. Chance, "A new double-tuned probed for concurrent 1H and 31P NMR," (in en), *Journal of Magnetic Resonance (1969),* vol. 65, no. 1, pp. 122-129, 1985-10-15 1985, doi: 10.1016/0022-2364(85)90380-4.

[4] C. H. Choi, S. M. Hong, Y. Ha, and N. J. Shah, "Design and construction of a novel (1)H/(19)F double-tuned coil system using PIN-diode switches at 9.4T," *J Magn Reson,* vol. 279, pp. 11-15, Jun 2017, doi: 10.1016/j.jmr.2017.04.005.

[5] C. H. Choi, S. M. Hong, J. Felder, and N. J. Shah, "The state-of-the-art and emerging design approaches of double-tuned RF coils for X-nuclei, brain MR imaging and spectroscopy: A review," *Magn Reson Imaging,* vol. 72, pp. 103-116, Oct 2020, doi: 10.1016/j.mri.2020.07.003.

[6] H. Lim, K. Thind, F. M. Martinez-Santiesteban, and T. J. Scholl, "Construction and evaluation of a switch-tuned 13C-1H birdcage radiofrequency coil for imaging the metabolism of hyperpolarized 13C-enriched compounds," *Journal of Magnetic Resonance Imaging,* vol. 40, no. 5, pp. 1082-1090, 2014-11-01 2014, doi: 10.1002/jmri.24458.

[7] C. P. Ambulo, S. Tasmim, S. Wang, M. K. Abdelrahman, P. E. Zimmern, and T. H. Ware, "Processing advances in liquid crystal elastomers provide a path to biomedical applications," *Journal of Applied Physics,* vol. 128, no. 14, p. 140901, 2020-10-14 2020, doi: 10.1063/5.0021143.

[8] L. Yang, K. Setyowati, A. Li, S. Gong, and J. Chen, "Reversible Infrared Actuation of Carbon Nanotube–Liquid Crystalline Elastomer Nanocomposites," *Adv. Mater.,* vol. 20, no. 12, pp. 2271-2275, 2008, doi: https://doi.org/10.1002/adma.200702953.

[9] D. M. Meng Wang, Chengjie Wang, "Near-Infrared Light Responsive Liquid Crystal Elastomers," *Progress in Chemistry,* vol. 32, no. 10, pp. 1452-1461, 2020-10-24 2020, doi: 10.7536/pc200335.

[10] M. O. Saed *et al.*, "Molecularly-Engineered, 4D-Printed Liquid Crystal Elastomer Actuators," *Advanced Functional Materials,* vol. 29, no. 3, p. 1806412, 2019-01-01 2019, doi: 10.1002/adfm.201806412.

[11] R. S. Kularatne, H. Kim, J. M. Boothby, and T. H. Ware, "Liquid crystal elastomer actuators: Synthesis, alignment, and applications," *Journal of Polymer Science Part B: Polymer Physics,* vol. 55, no. 5, pp. 395-411, 2017-03-01 2017, doi: 10.1002/polb.24287.

[12] S. Tasmim *et al.*, "Liquid crystal elastomer based dynamic device for urethral support: Potential treatment for stress urinary incontinence," *Biomaterials,* vol. 292, p. 121912, 2023/01/01/ 2023, doi: https://doi.org/10.1016/j.biomaterials.2022.121912.

[13] C. Wang *et al.*, "Soft Ultrathin Electronics Innervated Adaptive Fully Soft Robots," *Adv. Mater.,* vol. 30, no. 13, p. 1706695, 2018-03-01 2018, doi: 10.1002/adma.201706695.

[14] A. Kotikian, R. L. Truby, J. W. Boley, T. J. White, and J. A. Lewis, "3D Printing of Liquid Crystal Elastomeric Actuators with Spatially Programed Nematic Order," *Adv. Mater.,* vol. 30, no. 10, p. 1706164, 2018-03-01 2018, doi: 10.1002/adma.201706164.

[15] T. Carrell, R. Del Bosque, M. Wilcox, and M. McDougall, "A three-element triple-tuned array implemented with switchable matching and tuning," in *Proceedings of the 27th Annual International Society of Magnetic Resonance in Medicine Conference*, Montreal, CA, May 2019 2019.

[16] X. Lu *et al.*, "4D-Printing of Photoswitchable Actuators," *Angew Chem Int Ed Engl,* vol. 60, no. 10, pp. 5536-5543, Mar 1 2021, doi: 10.1002/anie.202012618.

[17] A. Ryabchun, Q. Li, F. Lancia, I. Aprahamian, and N. Katsonis, "Shape-Persistent Actuators from Hydrazone Photoswitches," *Journal of the American Chemical Society,* vol. 141, no. 3, pp. 1196-1200, 2019-01-23 2019, doi: 10.1021/jacs.8b11558.

[18] J. C. Rojas and F. Gonzalez-Lima, "Low-level light therapy of the eye and brain," (in eng), *Eye Brain,* vol. 3, pp. 49-67, 2011, doi: 10.2147/eb.S21391.

[19] D. Barolet, F. Christiaens, and M. R. Hamblin, "Infrared and skin: Friend or foe," *Journal of Photochemistry and Photobiology B: Biology,* vol. 155, pp. 78-85, 2016/02/01/ 2016, doi: https://doi.org/10.1016/j.jphotobiol.2015.12.014.

[20] R. J. Lanzafame, S. de la Torre, and G. H. Leibaschoff, "The Rationale for Photobiomodulation Therapy of Vaginal Tissue for Treatment of Genitourinary Syndrome of Menopause: An Analysis of Its Mechanism of Action, and Current Clinical Outcomes," (in eng), *Photobiomodul Photomed Laser Surg,* vol. 37, no. 7, pp. 395-407, Jul 2019, doi: 10.1089/photob.2019.4618.

[21] C. Ferraresi, Y.-Y. Huang, and M. R. Hamblin, "Photobiomodulation in human muscle tissue: an advantage in sports performance?," *Journal of Biophotonics,* vol. 9, no. 11-12, pp. 1273-1299, 2016-12-01 2016, doi: 10.1002/jbio.201600176.